

Article

Simulating Atmospheric Organic Aerosol in the Boreal Forest Using Its Volatility-Oxygen Content Distribution

Eleni Karnezi ^{1,†}, Liine Heikkinen ², Markku Kulmala ² and Spyros N. Pandis ^{1,3,4,*} ¹ Department of Chemical Engineering, Carnegie Mellon University, Pittsburgh, PA 15213, USA² Institute for Atmospheric and Earth System Research/Physics, Faculty of Science, University of Helsinki, 00014 Helsinki, Finland³ Department of Chemical Engineering, University of Patras, 26504 Patra, Greece⁴ Institute of Chemical Engineering Sciences, FORTH/ICEHT, 26504 Patra, Greece* Correspondence: spyros@chemeng.upatras.gr

† Current address: Earth Sciences Department, Barcelona Supercomputing Center, BSC-CNS, 08034 Barcelona, Spain.

Abstract: Various parameterizations of organic aerosol (OA) formation and its subsequent evolution in the two-dimensional Volatility Basis Set (2D-VBS) framework are evaluated using ground measurements collected in the 2013 PEGASOS field campaign in the boreal forest station of Hyytiälä in southern Finland. A number of chemical aging schemes that performed well in the polluted environment of the Po Valley in Italy during the PEGASOS 2012 campaign are examined, taking into account various functionalization and fragmentation pathways for biogenic and anthropogenic OA components. All seven aging schemes considered have satisfactory results, consistent with the ground measurements. Despite their differences, these schemes predict similar contributions of the various OA sources and formation pathways for the periods examined. The highest contribution comes from biogenic secondary OA (bSOA), as expected, contributing 40–63% depending on the modeling scheme. Anthropogenic secondary OA (aSOA) is predicted to contribute 11–18% of the total OA, while SOA from intermediate-volatility compounds (SOA-iv) oxidation contributes another 18–27%. The fresh primary OA (POA) contributes 4%, while the SOA resulting from the oxidation of the evaporated semivolatile POA (SOA-sv) varies between 4 and 6%. Finally, 5–6% is predicted to be due to long-range transport from outside the modeling domain.

Keywords: organic aerosol; 2D-VBS; aging parameterizations

Citation: Karnezi, E.; Heikkinen, L.; Kulmala, M.; Pandis, S.N. Simulating Atmospheric Organic Aerosol in the Boreal Forest Using Its Volatility-Oxygen Content Distribution. *Atmosphere* **2023**, *14*, 763. <https://doi.org/10.3390/atmos14050763>

Academic Editors: Longyi Shao and Long Peng

Received: 24 January 2023

Revised: 1 April 2023

Accepted: 20 April 2023

Published: 22 April 2023



Copyright: © 2023 by the authors. Licensee MDPI, Basel, Switzerland. This article is an open access article distributed under the terms and conditions of the Creative Commons Attribution (CC BY) license (<https://creativecommons.org/licenses/by/4.0/>).

1. Introduction

Atmospheric aerosols or particulate matter are liquid or solid airborne particles that are ubiquitous in the air that we breathe. They affect our lives by reducing visibility and influencing climate due to their reflection/absorption of incoming solar radiation and role in cloud formation [1]. Most importantly, they have serious adverse health effects including mortality and morbidity [2–4].

Organic aerosol (OA) is a major component of the sub-micrometer atmospheric particulate matter [5,6]. OA is either emitted directly into the atmosphere as particulate matter (primary OA, POA) or is formed by gas-to-particle conversion of volatile, intermediate-volatility and semi-volatile organic compounds (secondary OA, SOA). The corresponding oxidation reactions of organic compounds lead to thousands of mostly unknown oxygenated products. Our understanding of SOA formation mechanisms and physical properties remains incomplete.

Terrestrial vegetation emits a variety of biogenic volatile organic compounds into the atmosphere [7], some of which are subsequently oxidized, forming, among other products, secondary organic aerosols. Boreal forests produce a large amount of SOA mainly due to

emitted monoterpenes and sesquiterpenes [8]. The biogenic SOA fraction has been found to represent 10 to 65% of the measured OA in or near forested regions [9–12].

The use of lumped species allows the computationally efficient representation of OA in atmospheric chemical transport models (CTMs) [13]. The volatility basis set (VBS) framework [14] lumps organic compounds into surrogates along an axis of volatility. This approach typically employs species with effective saturation concentrations at 298 K separated by one order of magnitude, with values ranging from, say, 0.01 to $10^6 \mu\text{g m}^{-3}$. By quantifying the volatility distributions of primary and secondary OA, a physically reasonable, yet suitable for large-scale CTMs, description of semi-volatile organics can be obtained [15].

The VBS framework was extended [16,17] by adding a second dimension, the oxygen content (expressed as the O:C ratio), for the description of the OA chemical aging reactions [18,19] using a one-dimensional Lagrangian CTM (PMCAMx-Trj) as the host model for the simulations. PMCAMx-Trj simulates the chemical evolution of a column of air as it travels towards a user-selected receptor site. Using this 2D-VBS framework, various parameterizations for the OA processing and aging can be developed in an effort to describe the various functionalization and fragmentation chemical pathways of the reactions of the various organic compounds and the OH radicals or other oxidants. Murphy et al. [19] tested three alternative parameterizations for the functionalization processes. Two were relatively simple, assuming a net reduction of volatility by one or two orders of magnitude (corresponding to 1-bin and 2-bin shifts) during each aging reaction step. These reactions were accompanied by an increase of one or two atoms of oxygen with an equal probability. The third parameterization was more complex and was based on a detailed functionalization scheme introduced by Donahue et al. [16]. In this scheme, there is a 30%, 50% and 20% probability of adding 1, 2 or 3 oxygen atoms to the parent molecule, respectively. At the same time, each addition of oxygen atoms results in a different volatility reduction distribution, averaged to -1.75 in $\log_{10}C^*$ per oxygen group added. On the other hand, fragmentation is another important process that takes place during the chemical reactions of organic molecules with OH radicals, leading to products with lower carbon numbers than the precursors. Murphy et al. [19] assumed that this bond cleavage happens randomly and is uniformly distributed throughout the carbon backbone. Karnezi et al. [20] used the same Lagrangian CTM with the 2D-VBS framework and evaluated hundreds of different parameterizations of OA formation and chemical aging for the Po Valley in Italy during the PEGASOS 2012 campaign. They tested the full range of fragmentation probabilities varying from zero to unity, but assuming that the value remains constant in the chemical space. In reality, this probability is expected to depend on O to C ratios. Constant values were used to avoid the introduction of even more free parameters in the tested aging schemes [20]. The effect of the aging of biogenic SOA (bSOA) components was also tested in two different ways: assuming no net change in the volatility, as in previous applications with PMCAMx of Murphy and Pandis [21,22], and also assuming that bSOA follows similar aging pathways as anthropogenic SOA (aSOA) with a net reduction of volatility in every reaction step. The predictions of these parameterizations were compared against measurements of OA concentration and O:C both at the ground and aloft. The result of this exercise was the choice of seven “optimized” parameterizations that were all found to reproduce the available measurements in northern Italy well. Even if these parameterizations were quite different, their predictions about source contributions to the observed OA levels were relatively robust. However, it is not clear if these 2D-VBS parameterizations optimized for a polluted environment will perform well under different conditions, especially those that are quite different from the original polluted environment of the Po Valley.

A review of the current state of modeling of aerosol thermodynamics and mass transfer can be found in Semeniuk and Dastoor [23] and a review of the roles of semivolatile and intermediate-volatility organic compounds in SOA formation in Ling et al. [24].

In this work, we evaluate the same seven optimized chemical aging mechanisms in the 2D-VBS approach, suggested before [20] for the rural forested area of Hyytiälä in southern Finland during the PEGASOS campaign in 2013. Hyytiälä is representative of continental background boreal forest conditions and the model application on this area will allow the testing of the 2D-VBS in a clean environment that is dominated by biogenic emissions. This is an extreme test of the parameterizations, given the difference in conditions between one of the most polluted areas in Europe and the quite clean environment of the boreal forest.

2. Materials and Method

2.1. Site Description and Measurement Period

Measurements were performed at the Hyytiälä SMEAR II (Station for Measuring Forest Ecosystem—Atmosphere Relations) site during the PEGASOS 2013 campaign. The rural forested site [25] is in southern Finland (61°51' N, 24°17' E, 181 m above sea level), in the middle of a Scots pine forest. The nearest cities are: Tampere (235,000 inhabitants), located 50 km away to the southwest, and Jyväskylä (140,000 inhabitants), about 100 km away. There is also the town of Orivesi (population approximately 9000) 19 km south of SMEAR II and the nearby small village of Korkeakoski 6–7 km to the southeast of the station.

ACSM (Aerosol Chemical Speciation Monitor) measurements were performed at the ground during the campaign. A description of the ACSM and basic data processing can be found in Ng et al. [26]. The period of the measurements is from 23 April 2013 until 19 June 2013. This period was selected to achieve the objectives of the PEGASOS project regarding air quality–climate interactions, in this case, in a relatively clean environment dominated by biogenic emissions.

2.2. PMCAMx-Trj Model

We used the one-dimensional Lagrangian chemical transport model PMCAMx-Trj with the 2D-VBS module [18,19] simulating air parcels that arrived at Hyytiälä. The model solves the atmospheric general dynamic equation taking into account the relevant atmospheric processes: gas and aqueous-phase chemistry, atmospheric transport and turbulent dispersion, aerosol dynamics, dry and wet removal of gases and particles, inorganic and organic aerosol formation, and finally, area and point emissions from both anthropogenic and biogenic sources. Ten computational cells were used in this application with heights varying from 60 m near the ground to almost 3 km. An extended version of the SAPRC [27] chemical mechanism is used in this work for the simulation of gas-phase chemistry. The meteorological parameters (temperature, pressure, horizontal winds, clouds, water vapor, rainfall, vertical dispersion coefficients and land use) used as inputs in the model are provided by the Weather Research and Forecasting (WRF) model. The WRF simulation was periodically re-initialized (every 3 days) to ensure the accuracy of the inputs to the CTM. Area and point emissions were also provided by the inputs of the regular PMCAMx simulation for the European domain. This domain contains all of continental Europe, all the Mediterranean and parts of north Africa, Turkey and parts of Asia, Iceland and the North Sea as well as the western Atlantic. The approaches used for the estimation of the species' emission rates are the same as those described in Karnezi et al. [20]. The details of the emission inventory can be found in Fountoukis et al. [28] and implemented in the 2D-VBS framework with the Murphy et al. [18] method. The Model of Emissions of Gases and Aerosols from Nature (MEGAN) provides the emissions from terrestrial ecosystems. These are different for each simulation and vary with space and time [20]. Vertically resolved initial conditions and the top boundary conditions for PMCAMx-Trj were obtained from the corresponding output of the three-dimensional PMCAMx simulation for the same period of spring–early summer 2013.

2.3. Simulated Periods

The Hybrid Single Particle Lagrangian Integrated Trajectory (HYSPPLIT) model [29] was used to calculate 72 h back trajectories arriving at the receptor site of Hyytiälä. Six air parcels arriving at 3:00, 7:00, 11:00, 15:00, 19:00 and 23:00 local time (UTC + 2) in the ground forested site were simulated for 8 days (April 28, May 7, 11, 15 and 26 and June 9, 10 and 11). The air masses from the beginning of the campaign until the middle of May originated mostly from the Atlantic and arrived at Hyytiälä either directly from the west over Scandinavia or from the south, passing over the Baltic Sea. After mid-May, air masses started often from the east or northeast, either from the Arctic Ocean or from western Russia. During the last weeks, the situation changed again with air masses arriving from the Atlantic passing over Scandinavia. The current meteorological analysis is consistent with the conclusions of previous studies [30]. We selected days for which the trajectories at the different altitudes originated all from the same region. For consistency, we used the same WRF meteorological data as input to HYSPPLIT to calculate the back trajectories. Following Murphy et al. [18], the ensemble average of 20 trajectories with varied heights from 60 m up to 3 km is used, similarly to the application of PMCAMx-Trj in the Po Valley in Italy [20].

The twenty 72 h HYSPPLIT back trajectories arriving at Hyytiälä at 15:00 LT on 7 May 2013, are shown in Figure 1 as an example. They all originated from the eastern Atlantic Ocean, passed a day over the ocean and then over Ireland and the United Kingdom. During the next day they passed over the North Sea and Denmark. The air masses continued over Sweden and the Baltic Sea, and a few hours later arrived in the receptor site of Hyytiälä. The HYSPPLIT clustering analysis utility was used to estimate the average trajectory that was used in the simulations (Figure 1b).

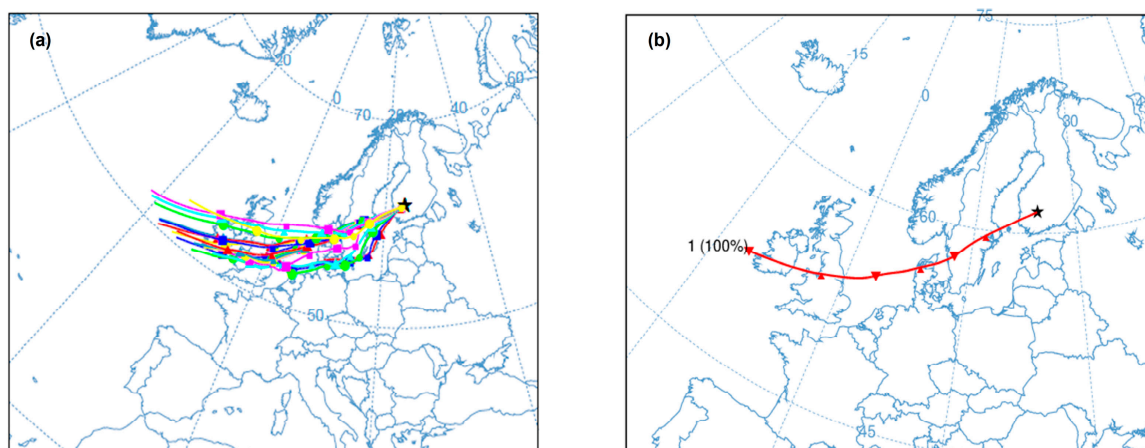


Figure 1. (a) The ensemble of 20 trajectories calculated by HYSPPLIT for air parcels arriving at the site of Hyytiälä on 7 May 2013 at 15:00 LT and (b) the ensemble average trajectory calculated by the HYSPPLIT clustering utility.

2.4. The Seven Aging Schemes

In the present simulations, we considered seven organic aerosol aging parameterizations, taking into account three different functionalization schemes, two biogenic SOA aging schemes and also different fragmentation probabilities. These parameterizations have been described in detail by Karnezi et al. [20] and they were determined to have the best performance in the OA simulations in the Po Valley in Italy. In the simulations here, the same parameterizations will be used to test their robustness when applied in a very different environment, i.e., the boreal forest in Finland. Table 1 summarizes the seven parameterizations that were used in the simulations.

Table 1. Characteristics of the seven parameterizations used in the current simulations.

| Parameterization Name | Functionalization Scheme | bSOA Increase during Aging | Fragmentation Probability (<i>b</i>) |
|-----------------------------|--------------------------|----------------------------|--|
| 1-bin | 1-bin | No | 0 |
| 1-bin/bSOA/ <i>b</i> = 0.15 | 1-bin | Yes | 0.15 |
| 2-bin | 2-bin | No | 0 |
| 2-bin/ <i>b</i> = 0.1 | 2-bin | No | 0.1 |
| 2-bin/bSOA/ <i>b</i> = 0.4 | 2-bin | Yes | 0.4 |
| DET/ <i>b</i> = 0.3 | DET | No | 0.3 |
| DET/bSOA/ <i>b</i> = 0.7 | DET | Yes | 0.7 |

The first set of simulations use the simple functionalization scheme (1-bin case), which assumes a one-volatility-bin reduction for every reaction with OH with a simultaneous increase in oxygen atoms, with a probability of 50% for an increase of one oxygen atom and 50% probability for an increase of two oxygen atoms. It also assumes negligible additional production of bSOA during aging (no bSOA aging) and no fragmentation of the organic compounds. Implicitly, this scheme assumes that the functionalization represents the net effect of these pathways.

The second set of simulations (1-bin/bSOA/*b* = 0.15 case) explores the role of fragmentation for the 1-bin simple functionalization scheme, assuming addition/production of bSOA during aging and combined with the fragmentation parameterization with the fragmentation probability equal to 15% as estimated previously [20].

The third set of simulations (2-bin case) uses the second simple functionalization scheme, where a two-volatility bin reduction is assumed for every reaction with a simultaneous increase in oxygen atoms. A 50% probability for the increase of one oxygen atom and 50% probability for the increase of two oxygen atoms are used similarly to the 1-bin case. Finally, there is no addition or production of bSOA, and fragmentation is neglected in this model.

The fourth set of simulations (2-bin/*b* = 0.1 case) uses the 2-bin functionalization scheme, neglecting bSOA aging and assuming now a fragmentation probability equal to *b* = 0.1 (10%) as estimated [20]. The fifth set of simulations (2-bin/bSOA/*b* = 0.4 case) uses the 2-bin functionalization, with the assumption of bSOA aging and more rapid fragmentation (*b* = 0.4).

In the sixth set of simulations, a more rigorous functionalization is explored, initially suggested by Donahue et al. [16], and which is called the detailed functionalization scheme. In this scheme, there is a 30% probability of adding one O atom, a 50% probability of adding two O atoms, and a 20% probability of adding three O atoms. Each addition of O atoms results in a different distribution of volatility reductions, with an average reduction of -1.75 in $\log_{10}C^*$ per oxygen added. It also assumes negligible additional production of bSOA during aging (no bSOA aging) and assumes a fragmentation probability equal to 30%, as estimated from the simulations in the Po Valley [20]. This case is called the DET/*b* = 0.3 case.

In the seventh and last simulation, the detailed functionalization, bSOA aging and intense fragmentation (*b* = 0.7) are assumed, and the case is called DET/bSOA/*b* = 0.7 case, as suggested by Karnezi et al. [20].

2.5. Performance Evaluation Metrics of Parameterizations

The performance of the seven different parameterizations used in the PMCAMx-Trj model is quantified in terms of the fractional error, the fractional bias, the absolute error, the absolute bias and the root mean square error, similarly to Karnezi et al. [20]. The equations that are used to calculate these performance metrics are shown below:

$$\text{Absolute Error} = \frac{1}{n} \sum_{i=1}^n |P_i - M_i| \quad (1)$$

$$\text{Absolute Bias} = \frac{1}{n} \sum_{i=1}^n (P_i - M_i) \quad (2)$$

$$\text{Fractional Error} = \frac{2}{n} \sum_{i=1}^n \frac{|P_i - M_i|}{(P_i + M_i)} \quad (3)$$

$$\text{Fractional Bias} = \frac{2}{n} \sum_{i=1}^n \frac{(P_i - M_i)}{(P_i + M_i)} \quad (4)$$

$$\text{Root Mean Square Error} = \sqrt{\frac{1}{n} \sum_{i=1}^n (P_i - M_i)^2} \quad (5)$$

where M_i is the measured value, P_i represents the corresponding model-predicted value, and n is the total number of data points. Hourly average values were used for all the days that were simulated.

3. Results

3.1. Simple Functionalization Scheme (1-Bin Case)

The first set of simulations used the simple functionalization scheme (1-bin), negligible additional production of bSOA during aging (no bSOA aging) and no fragmentation of the organic compounds. Implicitly, this scheme assumes that the simulated functionalization represents the net effect of these pathways. This scheme, until now, even though it is the simplest, has shown surprising success in all its previous applications [18–20].

The predicted average diurnal profile of OA mass concentration for the 1-bin scheme is shown in Figure 2. The average predicted OA is equal to $2.3 \mu\text{g m}^{-3}$ and the average measured OA mass concentration at the site was equal to $2.1 \mu\text{g m}^{-3}$ (Table 2). The measured OA concentrations during the PEGASOS campaign were quite typical for the season, even if significant intra-annual variability is observed in the site, as discussed in detail by Heikkinen et al. [31]. Once again, this simple aging scheme is the most successful of all parameterizations used in predicting the OA concentration (Table 2). It had the lowest root mean square error, as well as the lowest absolute bias (0.23) and one of the lowest fractional errors (38%). Most of the error is present during the first hours of the day when the model overpredicts the nighttime OA levels (Figure 2). The prediction skill metrics of the model 4-h average OA concentration against the average hourly ground measurements for the selected days during the PEGASOS 2013 campaign are summarized in Table 2. In Figure 3, the total average OA concentration is presented together with the OA composition predicted by all seven different parameterization schemes. Similarly to their application in the polluted Po Valley [20], the seven aging schemes predict similar average concentrations.

Table 2. Performance metrics of the seven parameterizations for hourly ground-level OA concentration. The measured average OA mass concentration was $2.1 \mu\text{g m}^{-3}$.

| 2D-VBS Parameterization | Predicted Average ($\mu\text{g m}^{-3}$) | Fractional Error | Fractional Bias | Absolute Error ($\mu\text{g m}^{-3}$) | Absolute Bias ($\mu\text{g m}^{-3}$) | Root Mean Square Error ($\mu\text{g m}^{-3}$) |
|----------------------------|--|---------------------|--------------------|--|---|---|
| 1-bin | 2.32 | 0.38 | −0.05 | 0.92 | 0.23 | 1.16 |
| 1-bin/bSOA/ $b = 0.15$ | 2.91 | 0.34 | 0.17 | 1.08 | 0.82 | 1.69 |
| 2-bin | 2.59 | 0.31 | 0.07 | 0.92 | 0.5 | 1.35 |
| 2-bin/ $b = 0.1$ | 2.46 | 0.34 | 0.02 | 0.91 | 0.38 | 1.25 |
| 2-bin/bSOA/ $b = 0.4$ | 2.98 | 0.31 | 0.22 | 1.06 | 0.90 | 1.67 |
| DET/ $b = 0.3$ | 2.45 | 0.33 | 0.02 | 0.89 | 0.36 | 1.21 |
| DET/bSOA/ $b = 0.7$ | 2.73 | 0.26 | 0.15 | 0.84 | 0.64 | 1.33 |

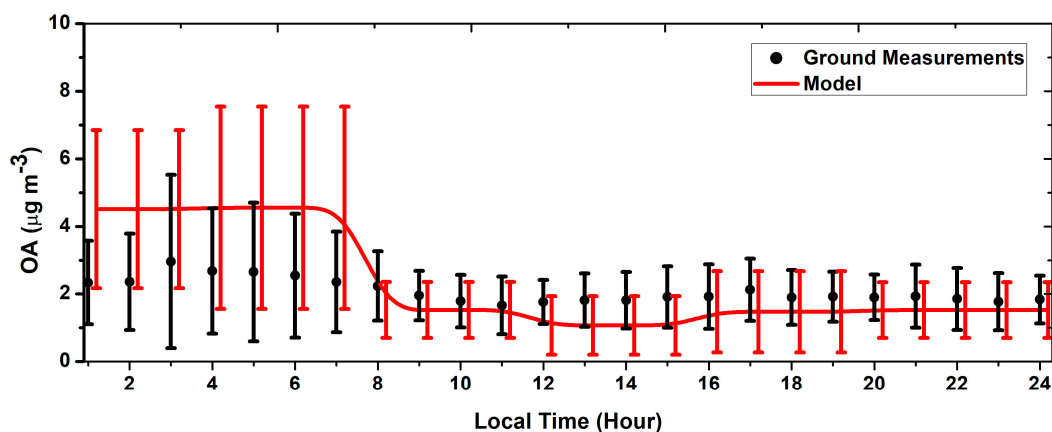


Figure 2. Average diurnal OA mass concentration at the ground level in Hyytiälä for the 1-bin simulation. The red line shows the model predictions and the black symbols represent the ACSM measurements. The error bars correspond to one standard deviation.

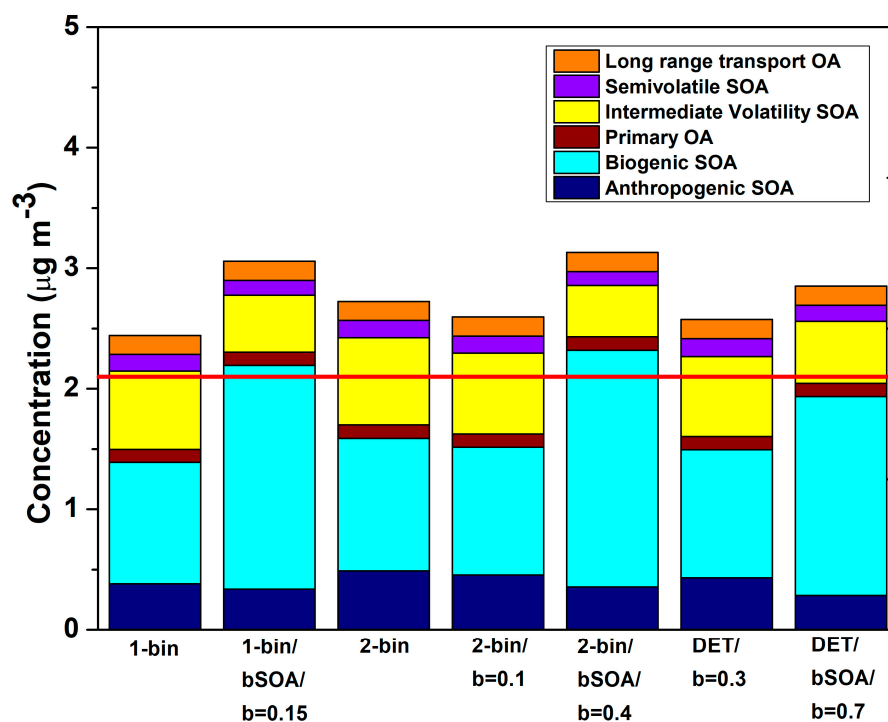


Figure 3. Predicted OA composition for the schemes with good performance for Hyytiälä. The red line indicates the average measured OA equal to $2.1 \mu\text{g m}^{-3}$.

Biogenic SOA dominates the predicted OA composition, as expected in a forested environment, contributing 41% of the total OA on average (Figure 4). Please note that the events simulated do not include stagnation periods during which the bSOA contribution should be much higher. The present results are not representative of the average conditions in Hyytiälä, but only of the limited periods simulated, which are dominated by transport. SOA from the oxidation of intermediate-volatility compounds contributed 27% according to PMCAMx-Trj and anthropogenic SOA from VOCs represented another 16%. The remaining material was fresh primary OA (4%), SOA from evaporation of the POA and subsequent oxidation (6%) and OA from long-range transport (6%).

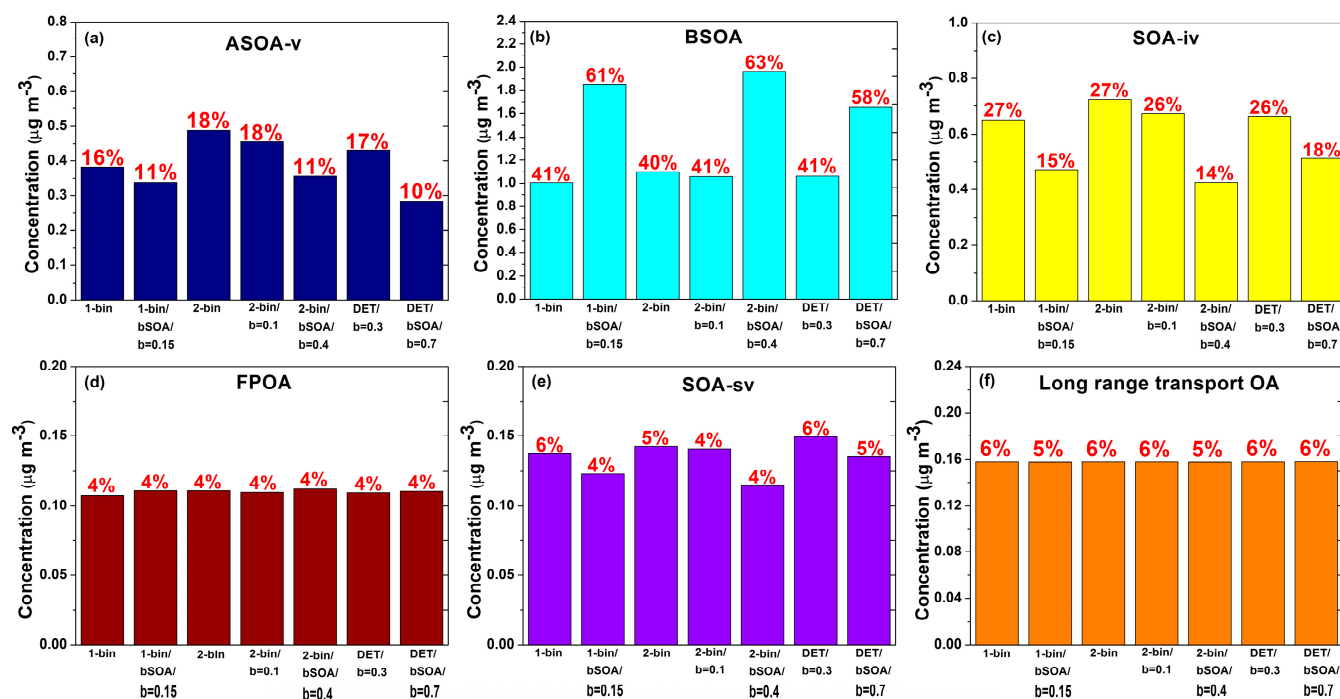


Figure 4. Predicted contribution of (a) ASOA-v, (b) BSOA, (c) SOA from oxidation of intermediate-volatility organic compounds, (d) FPOA, (e) SOA from oxidation of evaporated POA, and (f) OA from long-range transport using the seven aging parameterizations.

3.2. Evaluation of Aging Schemes

The second simple functionalization scheme (2-bin), assuming no addition or production of bSOA and neglecting fragmentation, resulted in a predicted average OA equal to $2.6 \mu\text{g m}^{-3}$ (Table 2). Its root mean square error was higher than that of the 1-bin case, its fractional bias was similar and its fractional error a little less. Overall, its performance was quite similar to that of the 1-bin scheme.

To explore the role of fragmentation, the 1-bin simple functionalization scheme was first used, assuming production of bSOA during aging combined with a fragmentation probability equal to 15% for all aging reactions as estimated previously [20]. The average predicted OA mass was equal to $2.9 \mu\text{g m}^{-3}$ with a fractional bias of 17% and a root mean square error equal to $1.69 \mu\text{g m}^{-3}$. This scheme tends to overpredict OA in contrast to the simple scheme, but the deterioration in performance is small to moderate.

The 2-bin functionalization scheme, neglecting bSOA aging and assuming a fragmentation probability $b = 0.1$, performed a little better (lower bias and root mean square error) than the 2-bin scheme. However, the improvements were small (reduction of bias by 5% and of root mean square error by $0.1 \mu\text{g m}^{-3}$) while the absolute error was almost the same. The 2-bin functionalization, with bSOA and more rapid fragmentation ($b = 0.4$), performed a little worse than the previous schemes with a tendency to overpredict OA (fractional bias 22%).

In the next set of simulations, the detailed functionalization scheme (DET case) was used, assuming a fragmentation probability equal to 30%. This scheme performed quite well with a fractional bias of only 2% and a fractional error of 33%. Its root mean square error was just $0.05 \mu\text{g m}^{-3}$ higher than that of the simple 1-bin scheme. Combining the detailed functionalization, bSOA aging and intense fragmentation ($b = 0.7$) reduced the fractional error to 26% but increased the bias to 15%.

Overall, the results are rather encouraging because the optimized schemes based on the Po Valley simulations appear to perform reasonably well in the very different environment of southern Finland.

For all three aging schemes, fragmentation of the organic molecules led to a better prediction of the OA concentration, while in some cases more fragmentation than the probabilities calculated previously [20] is probably needed.

3.3. Predicted OA Composition

The seven aging schemes proposed by Karnezi et al. [20] were the most successful ones in reproducing the OA measurements in the Po Valley in Italy and showed robust source contributions. Similarly, for the boreal forest in Finland all seven aging schemes once again predicted similar source contributions with some differences in the contribution of biogenic SOA varying from 40 to 63% of the total OA (Figure 4), depending on the parameterization scheme. The highest bSOA concentration was predicted by the aging schemes that assume production of bSOA during the aging reactions. The highest contribution (63%) was for the scheme assuming a 2-bin shift functionalization and fragmentation with 40% probability (2-bin/bSOA/ $b = 0.4$). The rest of the cases predicted lower bSOA levels, around 40% of the total.

SOA from anthropogenic VOC oxidation was predicted to contribute between 11 and 18% of the total OA (Figure 4). Its relatively low levels are consistent with the rural forested location of the boreal station of Hyytiälä. Most of the corresponding production took place elsewhere, and the resulting SOA was transported to the site.

SOA from the oxidation of intermediate-volatility compounds varied between 14 and 27%. The lowest contributions were predicted by the simulations that had high bSOA levels. The highest contributions (27%) were predicted by the simulations using the simple (1-bin) and faster (2-bin) functionalization scheme.

The fresh POA was 4% of the total OA, the SOA from the oxidation of evaporated POA 4–6%, and the OA from long-range transport 5–6%.

In general, all seven aging schemes were able to reproduce the variability and the average of the concentration of the OA.

4. Discussion

This study can be viewed as the next step of the effort to develop and test 2D-VBS schemes for the description of primary and secondary OA. In previous work [20], different types of parameterizations with different assumptions were optimized for the polluted conditions of the Po Valley in Italy. The Po Valley is dominated by anthropogenic emissions (transportation, industry, agriculture). In the present work, the robustness of the same optimized parameterizations has been tested when applied to a dramatically different environment usually dominated by biogenic emissions. By necessity, the modeling tools and necessarily the approach used are quite similar in the two steps. However, an important difference is that there is no effort here to optimize again the various parameterizations as done in the original work. The same parameterizations are used and tested.

The performance of the seven parameterizations was similar, leading to the conclusion that no parameterization was substantially superior. The simple schemes (1-bin and 2-bin) have the advantage that they can also be implemented in the 1D-VBS, with much lower computational cost. The other schemes cannot be easily simplified for the 1D-VBS without introduction of errors. Regarding the aging mechanisms, available findings suggest that there is significant later-generation production of SOA from anthropogenic precursors, while the corresponding later-generation production of SOA from biogenic precursors may be a lot smaller. These results, despite their uncertainty, suggest that one may need to treat the chemical aging of anthropogenic and biogenic compounds independently following previous modeling efforts. Furthermore, fragmentation of organic compounds during chemical aging is an important reaction pathway that should be included in some way in modeling efforts. The value of the use of the ensemble of the seven schemes in the present work is that they demonstrate which conclusions are robust and which are more uncertain (e.g., the contribution of biogenic SOA) and require additional testing with suitable field measurements.

The major difference of the schemes taking into account bSOA aging (cases 2, 5 and 7) from the rest is that they assume that the chemical aging reactions of the semivolatile biogenic SOA components lead to significant additional SOA formation. The other four schemes assume that in these reactions the fragmentation and functionalization of the biogenic SOA components balance each other and there is no change in total biogenic SOA mass. The other difference is fragmentation of the anthropogenic SOA components in these schemes. They assume fragmentation, which in turn results in reduction of the predicted anthropogenic SOA concentrations.

In the present study for the boreal forest, all seven models were able to reproduce the observed diurnal profile of the OA similarly to the study of the Po Valley. As expected, the biogenic SOA contribution (41–63% of the OA) for the boreal forest was significantly higher than in the Po Valley (17–45% of the OA) for all parameterizations. However, in both cases this was the most uncertain contribution of all components across the parameterizations. Additional studies to constrain this important OA component are needed.

5. Conclusions

The effects of different parameterizations of organic chemical aging processes of atmospheric organic compounds on organic aerosol (OA) concentration and chemical composition were investigated by using the two-dimensional Volatility Basis Set (2D-VBS) together with ground measurements in the boreal environment of Hyytiälä. The parameterizations used were the ones optimized for the Po Valley polluted environment by Karnezi et al. [20].

Despite the very different environment, the performance of all parameterizations was surprisingly good. The simple functionalization-only parameterization of Murphy et al. [18] had once again one of the best performances. This simple scheme appears for some reason that is not well understood to capture the behavior of OA in a lot of different environments, both rural and polluted. Its variation with a 2-bin change performed almost as well.

The fragmentation schemes with the probability values optimized for the Po Valley performed quite well in this case too. Increasing fragmentation rates are needed to “balance” the assumed net bSOA production during aging as the functionalization scheme becomes more aggressive.

Despite their differences, the seven schemes that performed well for OA predicted similar OA composition for the simulated period: 40–63% biogenic SOA, 11–18% SOA from anthropogenic VOCs, 14–27% SOA from IVOCs, 4% POA, 4–6% SOA from evaporated POA, and 5–6% from long-range transport. This agreement is encouraging about our ability to constrain the SOA sources, despite uncertainties about the details of the corresponding processes. These contributions are not representative of OA in the site in general but refer to the simulated periods that were dominated by transport. A rather surprising result of the current work is that the schemes perform well in this other extreme of air-quality conditions.

Author Contributions: Conceptualization, E.K. and S.N.P.; methodology, E.K., L.H. and M.K.; writing—original draft preparation, E.K.; writing—review and editing, E.K. and S.N.P., supervision, S.N.P. and M.K. All authors have read and agreed to the published version of the manuscript.

Funding: This research was supported by CHEVOPIN Project of the Hellenic Foundation for Research and Innovation (HFRI) under grant agreement no. 1819 and the PEGASOS project funded by the European Commission under the Framework Program 7 (FP7-ENV-2010-265148). We acknowledge the following projects: ACCC Flagship funded by the Academy of Finland grant number 337549, Academy professorship funded by the Academy of Finland (grant no. 302958).

Acknowledgments: We thank Mikael Ehn for assistance with the ground measurements. Support of the technical and scientific staff in Hyytiälä are acknowledged.

Conflicts of Interest: The authors declare no conflict of interest.

References

1. IPCC (Intergovernmental Panel on Climate Change). *Climate Change 2014: Mitigation of Climate Change*; Contribution of Working Group III to the Fifth Assessment Report of the Intergovernmental Panel on Climate Change; Cambridge University Press: Cambridge, UK; New York, NY, USA, 2014.
2. Nel, A. Air pollution-related illness: Effects of particles. *Science* **2005**, *308*, 804–806. [[CrossRef](#)] [[PubMed](#)]
3. Pope, C.A., III; Ezzati, M.; Dockery, D.W. Fine-particulate air pollution and life expectancy in the United States. *N. Engl. J. Med.* **2009**, *360*, 376–386. [[CrossRef](#)]
4. Caiazzo, F.; Ashok, A.; Waitz, I.A.; Yim, S.H.L.; Barrett, S.R. Air pollution and early deaths in the United States. Part I: Quantifying the impact of major sectors in 2005. *Atmos. Environ.* **2013**, *79*, 198–208. [[CrossRef](#)]
5. Zhang, Q.; Jimenez, J.L.; Canagaratna, M.R.; Allan, J.D.; Coe, H.; Ulbrich, I.; Alfarra, M.R.; Takami, A.; Middlebrook, A.M.; Sun, Y.L.; et al. Ubiquity and dominance of oxygenated species in organic aerosols in anthropogenically-influenced Northern Hemisphere midlatitudes. *Geophys. Res. Lett.* **2007**, *34*, L13801. [[CrossRef](#)]
6. Jimenez, J.L.; Canagaratna, M.R.; Donahue, N.M.; Prévôt, A.S.H.; Zhang, Q.; Kroll, J.H.; Decarlo, P.F.; Allan, J.D.; Coe, H.; Ng, N.L.; et al. Evolution of organic aerosols in the atmosphere. *Science* **2009**, *326*, 1525–1529. [[CrossRef](#)] [[PubMed](#)]
7. Guenther, A.; Hewitt, C.N.; Erickson, D.; Fall, R.; Geron, C.; Graedel, T.; Harley, P.; Klinger, L.; Lerdau, M.; McKay, W.A.; et al. A global model of natural volatile organic compound emissions. *J. Geophys. Res. Atmos.* **1995**, *100*, 8873–8892. [[CrossRef](#)]
8. Seinfeld, J.H.; Pandis, S.N. *Atmospheric Chemistry and Physics*, 2nd ed.; John Wiley and Sons: Hoboken, NJ, USA, 2006.
9. Szidat, S.; Ruff, M.; Perron, N.; Wacker, L.; Synal, H.-A.; Hallquist, M.; Shannigrahi, A.S.; Yttri, K.E.; Dye, C.; Simpson, D. Fossil and non-fossil sources of organic carbon (OC) and elemental carbon (EC) in Göteborg, Sweden. *Atmos. Chem. Phys.* **2009**, *9*, 1521–1535. [[CrossRef](#)]
10. Fu, P.; Kawamura, K.; Kanaya, Y.; Wang, Z. Contributions of biogenic volatile organic compounds to the formation of secondary organic aerosols over Mt. Tai, Central East China. *Atmos. Environ.* **2010**, *44*, 4817–4826. [[CrossRef](#)]
11. Schwartz, R.E.; Russell, L.M.; Sjostedt, S.J.; Vlasenko, A.; Slowik, J.G.; Abbatt, J.P.D.; Macdonald, A.M.; Li, S.M.; Liggio, J.; Toom-Sauntry, D.; et al. Biogenic oxidized organic functional groups in aerosol particles from a mountain forest site and their similarities to laboratory chamber products. *Atmos. Chem. Phys.* **2010**, *10*, 5075–5088. [[CrossRef](#)]
12. Finessi, E.; Decesari, S.; Paglione, M.; Giulianelli, L.; Carbone, C.; Gilardoni, S.; Fuzzi, S.; Saarikoski, S.; Raatikainen, T.; Hillamo, R.; et al. Determination of the biogenic secondary organic aerosol fraction in the boreal forest by NMR spectroscopy. *Atmos. Chem. Phys.* **2012**, *12*, 941–959. [[CrossRef](#)]
13. Pandis, S.N.; Harley, R.A.; Cass, G.R.; Seinfeld, J.H. Secondary organic aerosol formation and transport. *Atmos. Environ.* **1992**, *26*, 2266–2282. [[CrossRef](#)]
14. Donahue, N.M.; Robinson, A.L.; Stanier, C.O.; Pandis, S.N. Coupled partitioning, dilution, and chemical aging of semivolatile organics. *Environ. Sci. Technol.* **2006**, *40*, 2635–2643. [[CrossRef](#)] [[PubMed](#)]
15. Lane, T.E.; Donahue, N.M.; Pandis, S.N. Simulating secondary organic aerosol formation using the volatility basis-set approach in a chemical transport model. *Atmos. Environ.* **2008**, *42*, 7439–7451. [[CrossRef](#)]
16. Donahue, N.M.; Kroll, J.H.; Pandis, S.N.; Robinson, A.L. A two-dimensional volatility basis set: 1. Organic-aerosol mixing thermodynamics. *Atmos. Chem. Phys.* **2011**, *11*, 3303–3318. [[CrossRef](#)]
17. Donahue, N.M.; Kroll, J.H.; Pandis, S.N.; Robinson, A.L. A two-dimensional volatility basis set—Part 2: Diagnostics of organic-aerosol evolution. *Atmos. Chem. Phys.* **2012**, *12*, 615–634. [[CrossRef](#)]
18. Murphy, B.N.; Donahue, N.M.; Fountoukis, C.; Pandis, S.N. Simulating the oxygen content of ambient organic aerosol with the 2D volatility basis set. *Atmos. Chem. Phys.* **2011**, *11*, 7859–7873. [[CrossRef](#)]
19. Murphy, B.N.; Donahue, N.M.; Fountoukis, C.; Dall’Osto, M.; O’Dowd, C.; Kiendler-Scharr, A.; Pandis, S.N. Functionalization and fragmentation during ambient organic aerosol aging: Application of the 2-D volatility basis set to field studies. *Atmos. Chem. Phys.* **2012**, *12*, 10797–10816. [[CrossRef](#)]
20. Karnezi, E.; Murphy, B.N.; Poulain, L.; Herrmann, H.; Wiedensohler, A.; Rubach, F.; Kiendler-Scharr, A.; Mentel, T.F.; Pandis, S.N. Simulation of atmospheric organic aerosol using its volatility–oxygen-content distribution during the PEGASOS 2012 campaign. *Atmos. Chem. Phys.* **2018**, *18*, 10759–10772. [[CrossRef](#)]
21. Murphy, B.N.; Pandis, S. Simulating the formation of semivolatile primary and secondary organic aerosol in a regional chemical transport model. *Environ. Sci. Technol.* **2009**, *43*, 4722–4728. [[CrossRef](#)]
22. Murphy, B.N.; Pandis, S.N. Exploring summertime organic aerosol formation in the eastern United States using a regional-scale budget approach and ambient measurements. *J. Geophys. Res.* **2010**, *115*, D24216. [[CrossRef](#)]
23. Semeniuk, K.; Dastoor, A. current state of atmospheric aerosol thermodynamics and mass transfer modeling: A review. *Atmosphere* **2020**, *11*, 156. [[CrossRef](#)]
24. Ling, Z.; Wu, L.; Wang, Y.; Shao, M.; Wang, X.; Huang, W. Roles of semivolatile and intermediate-volatility organic compounds in secondary organic aerosol formation and its implication: A review. *J. Environ. Sci.* **2022**, *114*, 259–285. [[CrossRef](#)]
25. Hari, P.; Kulmala, M. Station for Measuring Ecosystem-Atmosphere Relations (SMEAR II). *Boreal Environ. Res.* **2005**, *10*, 315–322.
26. Ng, N.L.; Herndon, S.C.; Trimborn, A.; Canagaratna, M.R.; Croteau, P.; Onasch, T.M.; Sueper, D.; Worsnop, D.R. An Aerosol Chemical Speciation Monitor (ACSM) for routine monitoring of atmospheric aerosol composition. *Aerosol. Sci. Technol.* **2011**, *45*, 770–784. [[CrossRef](#)]

27. Carter, W.P.L. Programs and Files Implementing the SAPRC-99 Mechanism and Its Associated Emissions Processing Procedures for Models-3 and Other Regional Models. Available online: <https://intra.cert.ucr.edu/~carter/pubs/s99mod3.pdf> (accessed on 23 January 2023).
28. Fountoukis, C.; Racherla, P.N.; van der Gon, H.A.C.D.; Polymeneas, P.; Charalampidis, P.E.; Pilinis, C.; Wiedensohler, A.; Dall'Osto, M.; O'Dowd, C.; Pandis, S.N. Evaluation of a three-dimensional chemical transport model (PMCAMx) in the European domain during the EUCAARI May 2008 campaign. *Atmos. Chem. Phys.* **2011**, *11*, 10331–10347. [[CrossRef](#)]
29. Draxler, R.; Stunder, B.; Rolph, G.; Stein, A.; Taylor, A.; Zinn, S.; Loughner, C.; Crawford, A. *HYSPLIT4 User's Guide*; Version 5.2; 2022. Available online: https://www.arl.noaa.gov/documents/reports/hysplit_user_guide.pdf (accessed on 23 January 2023).
30. Nieminen, T.; Yli-Juuti, T.; Manninen, H.E.; Petäjä, T.; Kerminen, V.-M.; Kulmala, M. Technical note: New particle formation event forecasts during PEGASOS-Zeppelin Northern mission 2013 in Hyytiälä, Finland. *Atmos. Chem. Phys.* **2015**, *15*, 12385–12396. [[CrossRef](#)]
31. Heikkinen, L.; Äijälä, M.; Riva, M.; Luoma, K.; Dällenbach, K.; Aalto, J.; Aalto, P.; Aliaga, D.; Aurela, M.; Keskinen, H.; et al. Long-term sub-micrometer aerosol chemical composition in the boreal forest: Inter- and intra-annual variability. *Atmos. Chem. Phys.* **2020**, *20*, 3151–3180. [[CrossRef](#)]

Disclaimer/Publisher's Note: The statements, opinions and data contained in all publications are solely those of the individual author(s) and contributor(s) and not of MDPI and/or the editor(s). MDPI and/or the editor(s) disclaim responsibility for any injury to people or property resulting from any ideas, methods, instructions or products referred to in the content.